

# Wettability and Cell Viability in Uncoated Titanium Alloys

Renato Trevilato<sup>a\*</sup> , Kelli Cristina Micocci<sup>b</sup>, Débora Carneiro Moreira<sup>c</sup>,

Carlos Eiji Hirata Ventura<sup>a</sup> , Armando Ítalo Sette Antonialli<sup>a</sup> 

<sup>a</sup>Universidade Federal de São Carlos, Departamento de Engenharia Mecânica, São Carlos, SP, Brasil.

<sup>b</sup>Universidade Federal de São Carlos, Departamento de Química, São Carlos, SP, Brasil.

<sup>c</sup>Universidade de São Paulo, Escola de Engenharia de São Carlos, Departamento de Engenharia Mecânica, São Carlos, SP, Brasil.

Received: January 10, 2025; Revised: June 15, 2025; Accepted: June 29, 2025

The biological response to metallic biomaterials is strongly influenced by surface properties such as topography and wettability. This study evaluated the influence of roughness and contact angle on the cellular viability of pre-osteoblasts (MC3T3-E1) cultured on commercially pure titanium (grade 4), Ti-6Al-4V ELI, and Ti-12Mo-6Zr-2Fe (TMZF) alloy. Samples were machined by facing on a lathe using fixed parameters without coolant, and subsequently polished and characterized by confocal microscopy. Wettability tests were performed using the sessile drop method with varying droplet volumes and fitting methods using an optical tensiometer. Biological assays were conducted at 24, 48, and 72 hours using resazurin. Results showed that the combination of arithmetic roughness (0.6 and 1.3  $\mu\text{m}$ ) and hydrophilic behavior enhanced cell adhesion and proliferation, particularly on the TMZF alloy. Topographic symmetry ( $R_{sk}$ ) and kurtosis ( $R_{ku}$ ) were more strongly correlated with biological response than mean roughness ( $R_a$ ). The findings suggest that surface features and wettability properties act synergistically to modulate cell behavior and play a key role for biocompatibility and the development of optimized surfaces for biomedical applications.

**Keywords:** biomaterials, roughness, contact angle, pre-osteoblasts.

## 1. Introduction

The biocompatibility of metallic biomaterials is intrinsically related to their surface properties, including roughness, topography, and wettability. At the material–tissue interface, physical, chemical, and biological factors modulate the mechanisms of cell adhesion, proliferation, and differentiation, directly influencing bone–biomaterial integration, which is essential for the success of orthopedic and dental implants<sup>1-4</sup>.

Among the most used alloys, Ti-6Al-4V ELI ( $\alpha$ - $\beta$ ) stands out due to its machinability and mechanical performance, which favor its clinical use. However, this alloy contains vanadium (V) and aluminum (Al), elements associated with potential cytotoxic, carcinogenic, neurological, and inflammatory effects<sup>5-8</sup>.

As an alternative, commercially pure titanium (Ti-cp, grade 4), classified as a  $\alpha$ -phase alloy, offers excellent corrosion resistance due to the spontaneous formation of a passive oxide layer, an elastic modulus close to that of human bone, and good fracture toughness. Nevertheless, its low mechanical strength and limited response to heat treatments restrict its use in load-bearing implant applications<sup>9</sup>.

In this context,  $\beta$ -type titanium alloys such as Ti-12Mo-6Zr-2Fe (TMZF) and other TNZT-based variants have gained attention for being free of toxic elements and

exhibiting high biocompatibility, low stiffness, and superior mechanical properties<sup>4,5,10</sup>. With an elastic modulus similar to bone, these alloys reduce mechanical mismatch and promote enhanced physiological integration<sup>10,11</sup>. Additionally, they offer superior fatigue resistance and excellent tensile strength, reinforcing their potential in biomedical applications<sup>8,9</sup>.

Surface topographic features, such as average roughness ( $R_a$ ), skewness ( $R_{sk}$ ), and kurtosis ( $R_{ku}$ ), play a key role in cellular response. Surfaces with  $R_a$  values between 0.5 and 2.0  $\mu\text{m}$  enhance adhesion, proliferation, and differentiation of osteoblastic cells<sup>10</sup>, whereas excessive roughness can impair cell migration and fatigue resistance<sup>12,13</sup>. Recent studies show that  $R_{sk}$  and  $R_{ku}$  correlate more significantly with the formation of protein anchoring complexes (focal adhesions) and cellular behavior than  $R_a$  alone<sup>14</sup>.

Wettability is another critical factor in biological interaction. Hydrophilic surfaces ( $\theta < 90^\circ$ ) facilitate cell adhesion, whereas hydrophobic ones ( $\theta > 90^\circ$ ) may hinder osseointegration<sup>15-18</sup>. Surface modification techniques such as anodization, plasma oxidation, and deposition of bioactive coatings have been widely studied for their ability to enhance wettability and biological activity<sup>9,19,20</sup>.

Despite these advances, a gap remains in the literature regarding the relationship between the surface properties of uncoated  $\beta$ -type alloys and cellular response. Analyzing these surfaces in their machined state may yield data that are more representative of clinical applications. Therefore, this study aims to evaluate the influence of roughness and

\*e-mail: [rtrevilato@gmail.com](mailto:rtrevilato@gmail.com)

Associate Editor: Igor Vasconcelos.

Editor-in-Chief: Luiz Antonio Pessan.

wettability on the viability of pre-osteoblasts cultured on Ti-cp (grade 4), Ti-6Al-4V ELI, and Ti-12Mo-6Zr-2Fe (TMZF). The central hypothesis is that topographical and wettability variations induced by machining distinctly affect cellular behavior.

2. Materials and Methods

The metallic alloys used in this study were commercially obtained. Commercially pure titanium (grade 4), Ti-6Al-4V ELI, and Ti-12Mo-6Zr-2Fe (TMZF) alloys were supplied by the Department of Mechanical Engineering in the annealed condition, according to ASTM specifications<sup>21-23</sup>. No additional heat treatment was applied after machining, and all materials were kept in their original supplied condition.

The study was conducted in distinct stages (Figure 1), including sample fabrication, surface characterization, wettability evaluation, and biological assays. The samples were manufactured as small disks, 12.0 mm in diameter and 2.0 mm in thickness, obtained from annealed commercial cylindrical bars of the three alloys.

Machining was performed on a lathe, with a constant rotation of 300 rpm and variable feed rates of 0.038 mm/rev and 0.198 mm/rev, without the use of cutting fluids. A carbide inserts coated by chemical vapor deposition (CVD) with TiCrN, Al<sub>2</sub>O<sub>3</sub>, and TiN layers was used. This tool was selected

due to its high wear resistance and proven effectiveness in machining titanium alloys.

Following sample fabrication and prior to surface integrity characterization, metallographic and hardness tests were carried out to confirm the predominant microstructure in each sample:  $\alpha$ -phase in commercially pure titanium (grade 4),  $\alpha$ - $\beta$ -phase in Ti-6Al-4V ELI, and  $\beta$ -phase in Ti-12Mo-6Zr-2Fe (TMZF). Metallographic procedures followed the guidelines from the Metallography and Microstructures Handbook by the American Society for Metals – ASM<sup>24</sup>. Hardness tests were performed according to ASTM<sup>25,26</sup> and ISO<sup>27</sup> standards.

Next, the samples were manually ground using abrasive papers of 220, 320, 400, and 600 grits, followed by polishing with a 1  $\mu$ m alumina (Al<sub>2</sub>O<sub>3</sub>) solution on an Aeropol 2V polishing machine, with rotational speeds ranging from 0.5 to 600 rpm. All steps followed ASTM guidelines<sup>28,29</sup>.

Vickers hardness (HV) tests were conducted using a Heckert microhardness tester with an optical reading system (0.001 mm resolution). Indentations were made using a diamond pyramidal tip with a 136° face angle, applying a 30 kgf load for 15 seconds. Three measurements per sample were performed, and results were expressed as mean and standard deviation. The experimental hardness values were compared to ASTM reference ranges<sup>25,26</sup>, as shown in Table 1.

Subsequently, surface characterization was performed using confocal microscopy (Alicona Infinity Focus SL) to

Table 1. Comparison of Vickers hardness values for the analyzed samples and reference ranges.

Sample	Ti-cp	Ti-6Al-4V ELI	Ti-12Mo-6Zr-2Fe
Experimental value	186 ( $\pm$ 3.055)	337 ( $\pm$ 33.133)	316 ( $\pm$ 20.518)
Reference value <sup>25,26</sup>	200-250	330-400	250-350

Source: elaborated by the author.

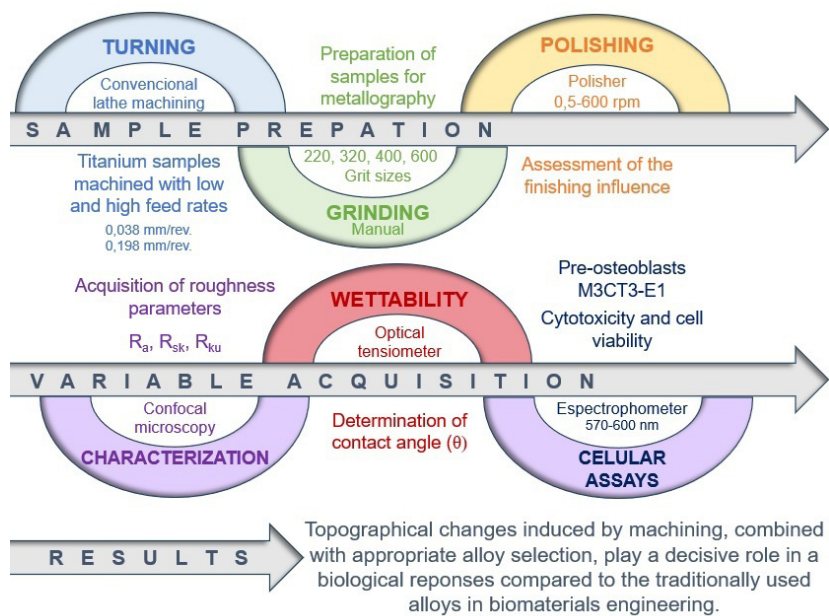


Figure 1. Flowchart of the experimental steps.

Source: created by the author.

evaluate mean roughness ( $R_a$ ), skewness ( $R_{sk}$ ), and kurtosis ( $R_{ku}$ ). These parameters were used to analyze profile symmetry and peak–valley distribution. For  $R_a$  values between 0.1  $\mu\text{m}$  and 2.0  $\mu\text{m}$ , a cut-off of 0.8 mm was used; for values above 2.0  $\mu\text{m}$ , a 2.5 mm cut-off was applied, in accordance with NBR ISO 4288<sup>30</sup>.

For each sample, three measurements of  $R_a$ ,  $R_{sk}$ , and  $R_{ku}$  were taken at distinct and random surface regions. Results were expressed as mean and standard deviation. Normal distribution was assumed based on the observed symmetry and the absence of significant outliers. Homogeneity of variances was verified using the F-test. Group comparisons were performed using analysis of variance (ANOVA) with a 5% significance level ( $p < 0.05$ ).

Among the surface integrity variables, roughness was selected as the primary parameter for comparative analysis. Localized surface defects, microstructural changes, or mechanical properties were not considered in this study.

Wettability tests were performed using a Kruss DAS25s optical tensiometer with the sessile drop technique, at room temperature (31 °C), with a dispensing rate of 3  $\mu\text{L/s}$  for distilled water. The contact angle ( $\theta$ ) was initially measured using a 5  $\mu\text{L}$  drop and different fitting methods. Subsequently, the droplet volume was varied from 5 to 80  $\mu\text{L}$  using the Young–Laplace equation. Tests were performed on both machined and polished surfaces to identify wettability patterns. Three random measurements were conducted for each condition, and results were expressed as mean and standard deviation.

Biological assays were conducted using pre-osteoblasts (MC3T3-E1) cultured in  $\alpha$ -MEM supplemented medium. Cells were incubated at 37 °C in a 5%  $\text{CO}_2$  atmosphere. Cell counting was performed using 0.4% Trypan Blue. Cell viability was assessed with the resazurin assay at 24, 48, and 72 hours. The reagent was prepared by mixing 10% non-reduced resazurin and 90% culture medium. Fluorescence readings were performed using a SpectraMax 190 spectrophotometer (570–600 nm). Resazurin is widely used in cytotoxicity, proliferation and cell viability assays, demonstrating mitochondrial metabolism<sup>31</sup>. All assays included a negative control (medium without cells) to correct background signals.

Cell cultures were conducted in 24-well plates in triplicate, distributed as follows: (i) wells with pre-osteoblasts only (control); (ii) wells with Ti-cp samples; (iii) wells with Ti-6Al-4V ELI samples; and (iv) wells with TMZF samples. After incubation with the reagent, 200  $\mu\text{L}$  aliquots from each well were transferred to 96-well plates for optical readings, maintaining a final cell concentration of approximately  $5 \times 10^4$  cells/mL, according to the standard protocol.

Additionally, cell adhesion assays were performed with different incubation periods to assess cell behavior in response to the different metallic surfaces. All data were statistically analyzed to validate the results.

### 3. Results and Discussion

Studies have shown that the surface morphology of materials significantly affects cellular behavior and responses<sup>32,33</sup>, particularly during the initial adhesion phase, which is considered the most critical biological phenomenon at the cell-implant interface. In addition to adhesion, subsequent

processes such as proliferation and differentiation are also affected and are essential for bone tissue formation<sup>34</sup>.

Turning was selected as the machining method due to its single point cutting nature and the continuity of the material removal process. Cutting speed plays a key role in surface finish, with variations being inherent to the fabrication process. Thus, distinct feed rates (low and high) were employed, justified by the potential formation of a built-up edge (BUE) near the center of the samples due to the lower cutting speed, which could increase surface roughness. It is worth noting that temperature was not monitored during the machining process.

According to Leite et al.<sup>35</sup>, evaluating a single roughness parameter is insufficient to properly characterize a surface, as distinct morphologies may present similar average roughness values. Therefore, it is necessary to correlate multiple rough parameters and consider additional factors that may influence the surface properties of biomaterials<sup>36</sup>.

The NBR ISO 4287 standard<sup>37</sup> defines the geometric parameters used in surface roughness measurement. In this study, roughness was adopted as the main variable of interest, focusing on the influence of machining feed rate on surface finish. It is important to note that potential microstructural changes induced during machining were not considered, as they were outside the study's scope.

Preliminary assays using fibroblasts on Ti-6Al-4V ELI samples showed that surfaces machined at low feed rates exhibited better cell adhesion and viability compared to those machined at high feed rates. These findings encouraged the inclusion of other titanium alloys widely used in biomedical applications, such as commercially pure titanium (grade 4) and the Ti-12Mo-6Zr-2Fe (TMZF) alloy for further tests with MC3T3-E1 pre-osteoblasts. Figure 2 illustrates the surface regions analyzed and the measurement line perpendicular to the machining marks.

The roughness analysis showed that, under low feed rate conditions, the peripheral regions had lower  $R_a$  values, except in the Ti-6Al-4V ELI alloy. Table 2 presents the average roughness values ( $R_a$ ) for each region and condition. Despite some variation, no statistically significant differences were found between measured regions ( $p$ -value  $> 0.05$ ).

Analysis of the  $R_{sk}$  parameter showed a predominance of wider peaks ( $R_{sk} < 0$ ) in the central regions of Ti-cp samples, while deeper valleys ( $R_{sk} > 0$ ) were observed in the TMZF and Ti-6Al-4V ELI alloys. However, no statistically significant differences were found ( $p$ -value  $> 0.05$ ). Regarding  $R_{ku}$ , Ti-cp and Ti-6Al-4V ELI showed distributions close to gaussian ( $R_{ku} \approx 3$ ), while TMZF showed higher peak/valley dispersion ( $R_{ku} > 3$ ), again with no statistical significance. ANOVA analysis (95% confidence level) supported the null hypothesis, suggesting that observed differences in  $R_a$ ,  $R_{sk}$ , and  $R_{ku}$  may be random.

Comparative tests between machined and polished surfaces showed that polishing significantly reduced  $R_a$  values, as shown in Table 3. However, ANOVA indicated that differences due to surface finish or alloy variation were not statistically significant ( $p$ -value  $> 0.05$ ). This reinforces the intrinsic heterogeneity of the analyzed surfaces.

Despite this, polishing resulted in greater variation in  $R_{ku}$ , suggesting inconsistencies associated with manual polishing. For polished surfaces, a  $R_{ku}$  below 3 is expected, indicating uniformity<sup>38,39</sup>. ANOVA showed that polishing had a significant

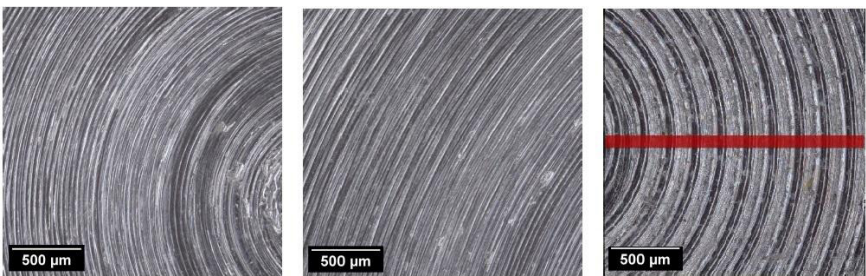


**Figure 2.** Confocal microscopy of the samples showing the measurement regions: central (a) and peripheral (b) and (c) shows the measurement line (100  $\mu\text{m}$  wide).  
**Source:** elaborated by the author.

**Table 2.**  $R_a$  values for Ti-cp, Ti-6Al-4V ELI, and Ti-12Mo-6Zr-2Fe alloys under low feed rate machining.

Measurement region	Ti-cp	Ti-6Al-4V ELI	Ti-12Mo-6Zr-2Fe
Central	1.387 ( $\pm$ 0.328)	1.020 ( $\pm$ 0.062)	0.920 ( $\pm$ 0.092)
Peripheral	0.780 ( $\pm$ 0.052)	1.300 ( $\pm$ 0.132)	0.660 ( $\pm$ 0.070)

**Source:** elaborated by the author.

**Table 3.**  $R_a$  values for Ti-cp, Ti-6Al-4V ELI, and Ti-12Mo-6Zr-2Fe alloys under machined and polished conditions.

Measurement region	Ti-cp	Ti-6Al-4V ELI	Ti-12Mo-6Zr-2Fe
Machined	0.780 ( $\pm$ 0.052)	1.300 ( $\pm$ 0.132)	0.660 ( $\pm$ 0.070)
Polished	0.163 ( $\pm$ 0.006)	0.123 ( $\pm$ 0.015)	0.173 ( $\pm$ 0.051)

**Source:** elaborated by the author.

effect on  $R_a$  ( $p < 0.05$ ), while the alloy type did not. It should be clarified that the arithmetic mean roughness values obtained characterize the roughness classes of the samples, being an important parameter of surface engineering applied to biomaterials.

According to NBR 8404<sup>40</sup>, turning processes can reach roughness classes N4 until N6 with “special care and methods,” and N7 until N10 under “usual conditions.” The experimental  $R_a$  values confirm the adequacy of the fabrication process for biomedical applications.

Liu et al.<sup>41</sup> emphasize that mechanical methods such as machining and polishing are effective in generating specific surface topographies that support cell adhesion. Chemical (e.g., acid/alkaline treatments, anodization) and physical (e.g., thermal spraying, plasma treatment) methods also improve corrosion and wear resistance, enhancing titanium alloys for biomedical use. These data highlight the diversity of treatments applied to titanium alloys with the aim of obtaining a surface suitable for osseointegration.

In wettability tests, machined surfaces of all three alloys showed predominantly hydrophilic behavior ( $\theta < 90^\circ$ ), except Ti-cp at a drop volume of 40  $\mu\text{L}$  (Figure 3). On the other hand, the polished surfaces of pure titanium and the Ti-6Al-4V ELI alloy presented a contact angle greater than  $90^\circ$ , indicating hydrophobic behavior, while the TMZF alloy remained hydrophilic in all conditions evaluated (Figure 4).

Although surface finish did not significantly influence contact angle ( $p > 0.05$ ), drop volume variation was statistically significant for polished surfaces. For machined surfaces, significance emerged only with  $\alpha = 10\%$ , indicating that drop volume may influence wettability under more flexible

criteria. Thus, it is possible to infer that the effect of the finishing of the different alloys does not directly interfere with the hydrophilicity of the alloys. However, on polished surfaces, especially under more flexible criteria at the significance level, the behavior of the samples becomes statistically relevant. Adjustment methods for contact angle analysis showed similar trends: machined surfaces remained hydrophilic (Figure 5), while polished surfaces tended to become hydrophobic (Figure 6), except for TMZF, which remained hydrophilic in all conditions. ANOVA confirmed that the adjustment method significantly affected wettability values. This result reinforces the need for standardization in the adjustment methodology, especially when comparing the finishing effect between different biomaterials.

Literature and additional experiments confirm that polished surfaces tend to reduce cell adhesion. Therefore, low-feed machined samples were used in the biological assays. After surface characterization, the mean arithmetic roughness obtained was  $R_a = 1.083 \mu\text{m}$  ( $\pm$  0.190  $\mu\text{m}$ ) for Ti-cp,  $R_a = 1.160 \mu\text{m}$  ( $\pm$  0.097  $\mu\text{m}$ ) for the Ti-6Al-4V ELI alloy and  $R_a = 0.790 \mu\text{m}$  ( $\pm$  0.081  $\mu\text{m}$ ) for the Ti-12Mo-6Zr-2Fe alloy. After cell seeding and incubation, fluorescence analysis revealed aerobic metabolic activity and overall viability. Since pre-osteoblasts tend to spread over the entire surface, no distinction between regions was made during biological analysis.

The combination of moderate roughness ( $R_a = 0.6\text{--}1.3 \mu\text{m}$ ) and hydrophilic behavior promoted better cell adhesion and viability<sup>11,14</sup>. These findings align with previous studies indicating that intermediate roughness and good wettability



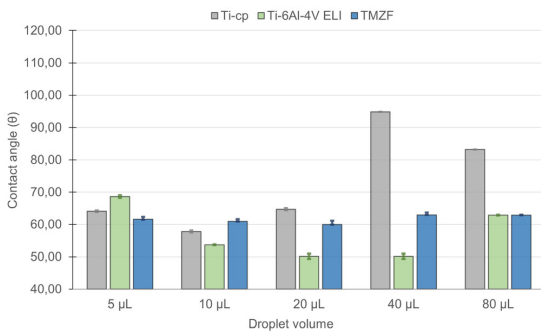


**Figure 3.** Graph showing droplet volume variation on machined surfaces.  
**Source:** elaborated by the author.

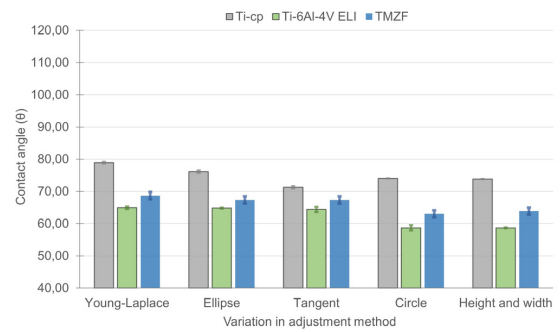


**Figure 5.** Graph showing the variation of adjustment method on machined surfaces.  
**Source:** elaborated by the author.

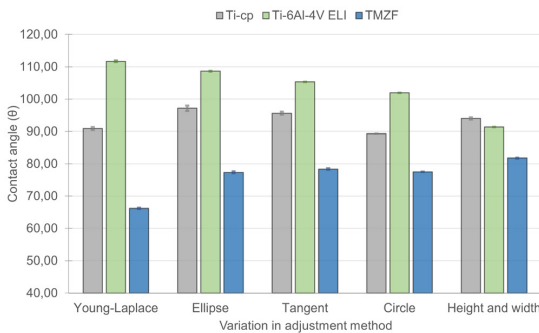


**Figure 4.** Graph showing droplet volume variation on polished surfaces.  
**Source:** elaborated by the author.

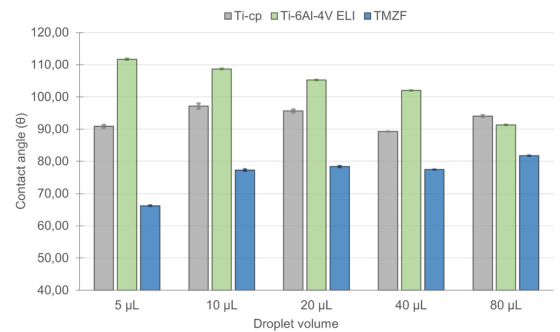


**Figure 6.** Graph showing the variation of adjustment methods on polished surfaces.  
**Source:** elaborated by the author.

support focal adhesion formation and osteogenic differentiation. Tuikampee et al.<sup>42</sup> also emphasized the synergistic effect of roughness and wettability on osteoblast adhesion.

Biological assays showed no cytotoxicity for any alloy. All samples exhibited increasing cell viability. Figure 7 shows viability over 24, 48, and 72 hours. TMZF showed the highest viability (36.83%), followed by Ti-cp (28.00%) and Ti-6Al-4V ELI (26.60%). The MC3T3-E1 cell line is well-established in viability studies.

The difference in performance between the alloys may be related to their microstructural characteristics. Pure titanium (grade 4) has a  $\alpha$ -microstructure, with compact hexagonal grains, which contributes to lower deformability and more stable roughness. The Ti-6Al-4V ELI alloy, in turn, with a two-phase structure ( $\alpha$ - $\beta$ ), has greater topographic heterogeneity, which may justify variations in the contact angle and lower cell viability. Finally, the TMZF alloy, predominantly  $\beta$ , has equiaxed and more homogeneous grains, which favors a lower modulus of elasticity and greater cell compatibility, as also reported by Wang et al.<sup>14</sup> and Hazwani et al.<sup>10</sup>. This evidence reinforces the influence of the crystalline phase and processing on the cell response.

The analysis of variance revealed statistically significant evidence against the null hypothesis, when considering the different alloys evaluated ( $p$ -value = 0.0097). The ANOVA demonstrates that the variations in the percentages of cell viability between the materials are statistically relevant. On the other hand, for the variable incubation time, the test did

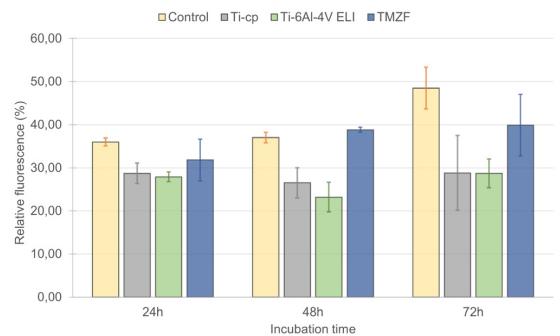


**Figure 7.** Graph showing cell viability (%) over 24, 48, and 72 hours for all alloys.  
**Source:** elaborated by the author.

not provide sufficient evidence to reject the null hypothesis ( $p$ -value = 0.1493), indicating that the differences observed between the times are within the expected variation.

Although this study used the resazurin assay to assess cell viability, the literature recommends complementary tests to expand the biological analysis of biomaterials. Proliferation assays such as MTT validate mitochondrial activity in a similar way<sup>43</sup>, while osteogenic differentiation methods with

markers such as ALP, RUNX2, and osteocalcin, in addition to gene expression analysis, contribute to investigating the osteoinductive potential of surfaces<sup>44,45</sup>. The adoption of these tests in future studies may enrich the understanding of the functional performance of titanium alloys.

Recent studies supported by finite element analysis have been used in the medical field to study biomechanical systems that present difficulties in simulating *in vivo* or *in vitro* responses, standing out as a valuable tool to examine the mechanical behavior of implants used in the dental field, allowing the evaluation of stress and deformation changes of the different components of the implant and the bone at a macroscopic level<sup>46,47</sup>.

Additionally, corrosion resistance is a property of great importance in the study of biomaterials, impacting both the biocompatibility and mechanical resistance of the implant. This fact can be explained by its close relationship with physiological fluids rich in chloride ions and, therefore, environments conducive to the development of corrosion processes. The evaluation of corrosion behavior is characterized as a qualification step in the development of a metallic material<sup>48</sup>.

Thus, the combination of hydrophilicity, topography and chemical composition has been shown to directly impact cellular behavior, suggesting that modulation of these factors can contribute to the development of more effective surfaces for biomedical applications. Although they were not evaluated in this study, microstructural changes resulting from machining, such as grain refinement, retained phases and residual stresses, can influence the cellular response, affecting local surface properties. This methodological limitation reinforces the importance of future studies that incorporate microstructural analysis, aiming at a more comprehensive understanding of the interaction between metallic biomaterials and bone tissue.

It is important to note that wear in biological environments was not evaluated in this study. However, its relevance is recognized, especially in environments rich in ions, such as in biological systems, where synergies between wear and corrosion can compromise the integrity of the implant. Therefore, it is proposed to carry out tribocorrosive tests and finite element modeling in future studies, aiming at a more comprehensive approach to the *in vivo* performance of the alloys investigated.

## 4. Conclusion

A comparative analysis of grade 4 commercially pure titanium, Ti-6Al-4V ELI alloy, and Ti-12Mo-6Zr-2Fe (TMZF) alloy showed that the surfaces machined at low feed presented consistent hydrophilic behavior, while the polished finish resulted in predominantly hydrophobic surfaces, except for the TMZF alloy, which remained hydrophilic under all conditions. The variation of the contact angle adjustment method demonstrated a significant influence on the characterization of wettability, especially on polished surfaces, highlighting the importance of methodological standardization in the evaluation of surface properties. The roughness parameters did not present statistically significant differences, however the data revealed lower average roughness values ( $R_a$ ) for pure titanium and for the TMZF alloy compared to the Ti-6Al-4V ELI alloy. Topographic analysis also indicated a marked dispersion in kurtosis ( $R_{ku}$ ) values after polishing, highlighting the limitation of the manual method in surface uniformity. In biological assays with pre-osteoblasts (MC3T3-E1), all alloys

showed high cell viability and absence of cytotoxicity. The TMZF alloy stood out with the highest mean cell viability, followed by pure titanium and Ti-6Al-4V ELI alloy, with statistically significant differences between the materials. These results suggest that the TMZF alloy, in addition to presenting favorable surface topography, has a high potential for osseointegration for implant applications, especially when used as machined. Thus, it is concluded that topographic modification by machining, combined with the appropriate choice of alloy, plays a determining role in the initial biological responses, with the TMZF alloy being a promising alternative to the alloys traditionally used in biomaterials engineering.

## 5. Acknowledgments

We would like to thank FAPESP (Processes 2015/15622-2 and 2022/06392-7), CAPES and the teams at UFSCar and USP for their technical and institutional support.

## 6. References

1. Ratner BD, Hoffman AS, Schoen FJ, Lemons JE, editors. Biomaterials science: an introduction to materials in medicine. 2. ed. Amsterdam: Elsevier; 2004.
2. Martins O. Estudo, *in vivo*, de uma hidroxiapatite de arquitetura otimizada [dissertation]. Coimbra: Universidade de Coimbra; 2009.
3. Ferreira ES. Interação da proteína albumina do soro bovino (BSA) com substratos sintéticos [thesis]. São Paulo: Universidade de São Paulo; 2010.
4. Chen L-Y, Cui Y-W, Zhang L-C. Recent development in beta titanium alloys for biomedical applications. *Metals*. 2020;10(9):1139. <http://doi.org/10.3390/met10091139>.
5. Saraiva EO, Almeida GS, Zambuzzi WF, Kuroda PAB, Grandini CR. Development of a novel  $\beta$ -type Zr-25Ta-5Ti alloy. *J Mater Eng Perform*. 2024;34:4765-73. <http://doi.org/10.1007/s11665-024-09473-9>.
6. Ponsionnet L, Comte V, Othmane A, Lagneau C, Charbonnier M, Lissac M, et al. Effect of surface topography and chemistry on adhesion, orientation and growth of fibroblasts on nickel-titanium substrates. *Mater Sci Eng C*. 2002;21(1-2):157-65. [http://doi.org/10.1016/S0928-4931\(02\)00097-8](http://doi.org/10.1016/S0928-4931(02)00097-8).
7. Corrêa DOG. Citotoxicidade de novas ligas à base de titânio visando aplicações biomédicas [dissertation]. Ilha Solteira: Universidade Estadual Paulista; 2022.
8. Zhang H, Wu Z, Wang Z, Yan X, Duan X, Sun H. Advanced surface modification techniques for titanium implants: a review of osteogenic and antibacterial strategies. *Front Bioeng Biotechnol*. 2025;13:1549439. <http://doi.org/10.3389/fbioe.2025.1549439>.
9. Balazic M, Kopac J, Jackson MJ, Ahmed W. Titanium and titanium alloy applications in medicine. *IJNB*. 2007;1(1):3-34. <http://doi.org/10.1504/IJNB.2007.016517>.
10. Hazwani MRSN, Lim LX, Lockman Z, Zuhailawati H. Fabrication of titanium-based alloys with bioactive surface oxide layer as biomedical implants: opportunity and challenges. *Trans Nonferrous Met Soc China*. 2022;32(1):1-44. [http://doi.org/10.1016/S1003-6326\(21\)65776-X](http://doi.org/10.1016/S1003-6326(21)65776-X).
11. Shi R, Hayashi K, Bang LT, Ishikawa K. Effects of surface roughening and calcite coating of titanium on cell growth and differentiation. *J Biomed Mater Res B Appl Biomater*. 2020;108(5):1943-51.
12. José GA. Análise comparativa do desempenho mecânico de ligas  $\beta$ -Ti em implantes ortopédicos como alternativas aos biomateriais metálicos comerciais [dissertation]. São Carlos: Universidade Federal de São Carlos; 2022.
13. Ponsionnet L, Reybier K, Jaffrezic N, Comte V, Lagneau C, Lissac M, et al. Relationship between surface properties (roughness, wettability) of titanium and titanium alloys and cell behaviour.

- Mater Sci Eng C. 2003;23(4):551-60. [http://doi.org/10.1016/S0928-4931\(03\)00033-X](http://doi.org/10.1016/S0928-4931(03)00033-X).
14. Wang S, Zhang M, Liu L, Xu R, Huang Z, Shi Z, et al. Femtosecond laser treatment promotes the surface bioactivity and bone ingrowth of Ti6Al4V bone scaffolds. *Sci Rep*. 2022;12:9537.
  15. Lampin M, Warocquier-Clérout R, Legris C, Degrange M, Sigot-Luizard MF. Correlation between substratum roughness and wettability, cell adhesion, and cell migration. *J Biomed Mater Res*. 1997;36(1):99-108. [http://doi.org/10.1002/\(SICI\)1097-4636\(199707\)36:1<99::AID-JBM12>3.0.CO;2-E](http://doi.org/10.1002/(SICI)1097-4636(199707)36:1<99::AID-JBM12>3.0.CO;2-E).
  16. Ramanathan R. Modificação da superfície de materiais para super-hidrofobicidade e hidrofiliçidade [thesis]. Belo Horizonte: Universidade Federal de Minas Gerais; 2012.
  17. Eriksson C, Nygren H, Ohlson K. Implantation of hydrophilic and hydrophobic titanium discs in rat tibia: cellular reactions on the surfaces during the first 3 weeks in bone. *Biomaterials*. 2004;25(19):4759-66. <http://doi.org/10.1016/j.biomaterials.2003.12.006>.
  18. Alencar AC. Estudo das modificações na superfície do titânio comercialmente puro e da liga Ti-6Al-4V usados como biomateriais utilizando-se deposição por plasma spray [dissertation]. Guaratinguetá: Universidade Estadual Paulista; 2002.
  19. Luo R, Jiao Y, Zhang S, Wu J, Wu X, Lu K, et al. Fabrication, properties and biological activity of a titanium surface modified with zinc via plasma electrolytic oxidation. *Front Mater*. 2023;10:1202110. <http://doi.org/10.3389/fmats.2023.1202110>.
  20. Shao L, Du Y, Dai K, Wu H, Wang Q, Liu J, et al.  $\beta$ -Ti alloys for orthopedic and dental applications: A review of progress on improvement of properties through surface modification. *Coatings*. 2021;11(12):1446. <http://doi.org/10.3390/coatings11121446>.
  21. ASTM: American Society for testing and Materials. ASTM F136-13: standard specification for wrought titanium-6aluminum-4vanadium ELI alloy for surgical implant applications. West Conshohocken, PA: ASTM International; 2013; 3 p.
  22. ASTM: American society for Testing and Materials. ASTM F67-13: standard specification for unalloyed titanium, for surgical implant applications. West Conshohocken, PA: ASTM International; 2017. 3 p.
  23. ASTM: American Society for Testing and Materials. ASTM F1813-21: standard specification for wrought titanium-12molybdenum-6zirconium-2iron alloy for surgical implant applications. West Conshohocken, PA: ASTM International; 2021. 5 p.
  24. Vander Voort GF, editor. Metallography and microstructures. Materials Park, OH: ASM International; 2004. (vol. 9). <http://doi.org/10.31399/asm.hb.v09.9781627081771>.
  25. ASTM: American Society for Testing and Materials. ASTM E384-22: standard test method for microindentation hardness of materials. West Conshohocken, PA: ASTM International; 2022.
  26. ASTM: American Society for Testing and Materials. ASTM E92-17: standard test methods for Vickers hardness and Knoop hardness of metallic materials. West Conshohocken, PA: ASTM International; 2017.
  27. ISO: International Organization for Standardization. ISO 6507-1: metallic materials: vickers hardness: part 1: test method. Geneva: ISO; 2005. 12 p.
  28. ASTM: American Society for Testing and Materials. ASTM E3-11: standard guide for preparation of metallographic specimens. West Conshohocken, PA: ASTM International; 2011.
  29. ASTM: American Society for Testing and Materials. ASTM E407-07(2015): standard practice for microetching metals and alloys. West Conshohocken, PA: ASTM International; 2015.
  30. ABNT: Associação Brasileira de Normas Técnicas. ABNT NBR ISO 4288: especificações geométricas do produto (GPS): rugosidade: método do perfil: regras e procedimentos para avaliação de rugosidade. Rio de Janeiro: ABNT; 2008. 10 p.
  31. Rolón M, Vega C, Escario JA, Gómez-Barrio A. Development of resazurin microtiter assay for drug sensibility testing of *Trypanosoma cruzi* epimastigotes. *Parasitol Res*. 2006;99(2):103-7. <http://doi.org/10.1007/s00436-006-0126-y>.
  32. Xavier SP, Carvalho PSP, Beloti MM, Rosa AL. Response of rat bone marrow cells to commercially pure titanium submitted to different surface treatments. *J Dent*. 2003;31(3):173-80. [http://doi.org/10.1016/S0300-5712\(03\)00027-7](http://doi.org/10.1016/S0300-5712(03)00027-7).
  33. Suh J-Y, Jang B-C, Zhu X, Ong JL, Kim K. Effect of hydrothermally treated anodic oxide films on osteoblast attachment and proliferation. *Biomaterials*. 2003;24(2):347-55. [http://doi.org/10.1016/S0142-9612\(02\)00325-3](http://doi.org/10.1016/S0142-9612(02)00325-3).
  34. Deligianni DD, Katsala N, Ladas S, Sotiropoulou D, Amedee J, Missirlis YF. Effect of surface roughness of the titanium alloy Ti-6Al-4V on human bone marrow cell response and on protein adsorption. *Biomaterials*. 2001;22(11):1241-51. [http://doi.org/10.1016/S0142-9612\(00\)00274-X](http://doi.org/10.1016/S0142-9612(00)00274-X).
  35. Leite GB, Fonseca YR, Elias CN, Gomes AV. Relação entre os parâmetros de rugosidade 3D e a molhabilidade do titânio com grãos micrométricos e sub-micrométricos. *Matéria*. 2020;25(2):e12655.
  36. Elias CN. Factors affecting the success of dental implants. In: Turkyilmaz I, editor. *Implant dentistry: a rapidly evolving practice*. Rijeka: InTech; 2011. p. 319-64.
  37. ABNT: Associação Brasileira de Normas Técnicas. ABNT BR ISO 4287: especificações geométricas do produto (GPS): rugosidade: método do perfil: termos, definições e parâmetros da rugosidade. Rio de Janeiro: ABNT; 2002. 18 p.
  38. Moreto FAL. Análise de componentes independentes aplicada à separação de sinais de áudio [thesis]. São Paulo: Universidade de São Paulo; 2008.
  39. Moreira LS. A relação parabólica entre assimetria e curtose em um experimento de gasificador fluidizado [dissertation]. Brasília: Universidade de Brasília; 2019.
  40. ABNT: Associação Brasileira de Normas Técnicas. ABNT NBR 8404: indicação do estado de superfícies em desenhos técnicos. Rio de Janeiro: ABNT; 1984. 10 p.
  41. Liu X, Chu PK, Ding C. Surface modification of titanium, titanium alloys, and related materials for biomedical applications. *Mater Sci Eng R*. 2004;47(3-4):49-121.
  42. Tuikampee S, Chaijareenont P, Rungsiyakul P, Yavirach A. Titanium surface modification techniques to enhance osteoblasts and bone formation for dental implants: a narrative review on current advances. *Metals*. 2024;14(5):515. <http://doi.org/10.3390/met14050515>.
  43. Alves EGL, Serakides R, Rosado IR, Pereira MM, Ocarino NM, Oliveira HP, et al. Efeito do produto iônico do biovidro 60S na diferenciação osteogênica de células-tronco mesenquimais do tecido adiposo de cães. *Arq Bras Med Vet Zootec*. 2015;67(4):969-78. <http://doi.org/10.1590/1678-4162-7539>.
  44. Gasparoni LM. Osteogênese in vitro a partir de células-tronco mesenquimais humanas cultivadas em scaffolds de quitosana e hidroxiapatita [dissertation]. Ribeirão Preto: Universidade de São Paulo; 2017. 123 p.
  45. Silva AF. Avaliação da resposta celular a biomateriais para fins de engenharia tecidual óssea [dissertation]. Natal: Universidade Federal do Rio Grande do Norte; 2018. 98 p.
  46. Falcinelli C, Valente F, Vasta M, Traini T. Finite element analysis in implant dentistry: state of the art and future directions. *Dent Mater*. 2023;39(6):539-56. <http://doi.org/10.1016/j.dental.2023.04.002>.
  47. Fernández BV. Evaluación del efecto de la razón corona-implante en la distribución de esfuerzos en implantes dentales por Método de los Elementos Finitos [trabajo de grado]. Antioquia: Universidad EIA; 2024.
  48. Assis SL. Investigação da resistência à corrosão da liga Ti-13Nb-13Zr por meio de técnicas eletroquímicas e de análise de superfície [thesis]. São Paulo: Universidade de São Paulo; 2006. [Portuguese]

## Data Availability

The full dataset supporting the findings of this study is available upon request to the corresponding author (Renato Trevilato, [rtrevilato@gmail.com](mailto:rtrevilato@gmail.com))